Anomalous $L\gamma_{2,3}$ x-ray emission spectrum of Xe

M. Ohno*
Institute of Theoretical Physics, Chalmers University of Technology, S-412 96 Göteborg, Sweden

R. E. LaVilla
National Bureau of Standards, Gaithersburg, Maryland 20899
(Received 14 March 1988)

The $L\gamma_{2,3}(2s^{-1}\rightarrow 4p^{-1})$ x-ray emission spectrum of gaseous xenon was measured in fluorescence with a high-resolution vacuum double-crystal spectrometer. The spectrum was also calculated by the Green's-function method. The agreement is excellent. It is shown that the spectrum can be interpreted essentially in terms of the spectral function of the $4p$ hole. The effects of the initial $2s$-hole state on the final $4p$-hole state are small. The spectrum shows that the quasiparticle picture of a $4p$ hole in xenon breaks down because of strong $4p^{-1}\leftrightarrow 4d^{-2}4(n,\varepsilon)f$ super-Coster-Kronig processes.

I. INTRODUCTION

The problem of a discrete level interacting with a continuum, namely, a core hole created by electron impact or photoionization which subsequently autoionize via Auger transitions, is well known. In general, the Auger transition is a very weak process so that the electronic charge density surrounding the core hole is not distorted. However, a similar kind of transition process associated with the creation of a core hole can be so strong that the charge density surrounding the core hole will be distorted and as a result the core-hole energy can exhibit large shifts and the decay rate can be greatly modified. In other words, when the single-hole level and the continuum are strongly coupled to each other, the quasiparticle picture of the core hole can break down.[1] Examples of this have been found in the core levels of intermediate-atomic-number elements and more complex systems such as molecules.[2,3] In the case of atomic systems examples were found in the x-ray photoelectron spectroscopy (XPS) spectra, x-ray emission spectroscopy (XES) spectra and Auger electron spectroscopy (AES) spectra of atomiclike systems.[4–10]

The most spectacular examples found so far are the XPS, XES, and AES spectra of the atomic elements from Pd ($Z=46$) to Xe ($Z=54$) which involve the $4p$ core-hole level.[4–10] These spectra have been also studied theoretically by the Green's-function method.[5,6,8–10] It has been shown that the quasiparticle picture of a $4p$ hole breaks down due to strong coupling between the $4p$ core-hole level and $4d$ double-hole continuum, namely, a $4p^{-1}\leftrightarrow 4d^{-2}n(\varepsilon)f$ super-Coster-Kronig process.[5–10] In a previous work the $L\gamma_{2,3}(2s^{-1}\rightarrow 4p^{-1})$ XES spectra of the elements Sn ($Z=50$), Te ($Z=52$), and I ($Z=53$) were measured.[7] These XES spectra have much less inelastic background than the XPS spectrum which has a very large background. For a comparison with the theoretical spectrum, the XES spectrum is much more useful than the corresponding XPS spectrum.[5–7]

In the present work, we present the $L\gamma_{2,3}$ XES spectrum of Xe, which is measured for the first time as part of a series of experimental and theoretical studies of the $L\gamma_{2,3}$ XES spectra of elements ranging from Xe ($Z=54$) to Eu ($Z=63$), where the $4f$ level starts to be filled and the quasiparticle picture of a $4p$ hole begins to be valid. The analysis of the spectra of the elements Ba ($Z=56$) to Eu ($Z=63$) is more complicated and we leave that to a forthcoming paper.

The overall shape of the $L\gamma_{2,3}$ XES spectrum of Xe measured in the present work is similar to that of the $4p$ XPS spectrum of Xe.[4] We calculated also the $L\gamma_{2,3}$ XES spectrum of Xe by the Green's-function method. Although in the present work we neglected the memory effects of the $2s$ hole on the final hole state (namely, the vertex corrections), we obtained excellent agreement with experiment. The present theoretical study shows that the $L\gamma_{2,3}$ XES spectrum of Xe can be described essentially in terms of the spectral function of the final $4p$ hole and can be interpreted in the same way as the $4p$ XPS spectrum of Xe.

II. EXPERIMENTAL

The fluorescent xenon $L\gamma_{2,3}$ XES spectrum was measured on a vacuum double-crystal spectrometer[11] using Ge(220) crystals ($2d=4.000\,6754$ Å at 22.5 °C.[12] Commercial CP-grade xenon gas was contained in a fluorescence cell[13] by 25-μm-thick beryllium windows at a pressure of 0.13 kPa (100 Torr). The primary exciting radiation was from a high-power x-ray tube[14] with a cobalt-plated copper anode operating at 13 kV, 190 mA. The monochromatized radiation from xenon was detected with a gas-flow proportional counter filled with P-10 (90% argon, 10% methane) at a pressure of 0.92 kPa (700 Torr). The spectrum was obtained by step-scanning the second crystal. The dwell time was 6.8 min/point with a count rate of 0.6 counts/sec at the peak.

The experimental spectrum in Fig. 1, above 5281 eV is the average of seven scans. Below 5281 eV, where the data have more scatter, only two scans were averaged.

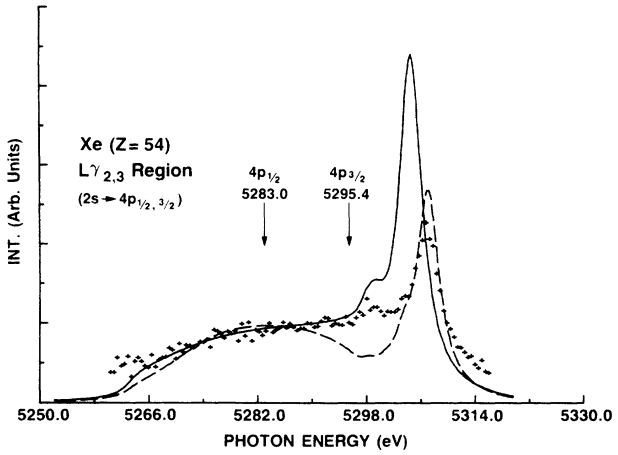

FIG. 1. The symbol (+) is the experimental XES of gaseous xenon in the $L\gamma_{2,3}(2s \rightarrow 4p_{1/2,3/2})$ region. The dashed line is the calculated spectral distribution using approximation 1. The solid line is approximation 5 and is similar to approximations 2–4. Also indicated are the calculated positions of the $2s \rightarrow 4p_{1/2,3/2}$ lines using the Dirac-Hartree-Fock ΔSCF $4p$-hole energies and the experimental $2s$-hole energy (5452.2 eV) as determined in this work.

Corrections[15] for crystal temperature, vertical divergence, and index of refraction were applied to determine the Bragg angle. The uncertainty of the experimental energy scale of ±0.04 eV is primarily due to counting statistics and modelling of the spectral lines. The xenon $L\gamma_{2,3}$ peak position is 5306.7±0.2 eV. The FWHM of the peak is 4.2±0.4 eV. The diffraction rocking curve had a FWHM of 0.50±0.03 eV.

III. THEORY

In previous work[6,16] it is shown that when one neglects the effects of the initial hole state, one obtains the following expression for the x-ray emission process $i^{-1} \rightarrow f^{-1} + \hbar\omega$ by treating the primary ionization and the secondary emission processes as a single one-step process:

$$I^{x}(\omega) \propto \omega^3 \int dE \, |\langle i \,|\, Z \,|\, \varepsilon \rangle|^2 \frac{\pi \, |g_{if}(\omega)|^2}{\mathrm{Im}\Sigma_i(E)} \times A_i(E) A_f(E+\omega) \, , \tag{1}$$

where Z is the dipole moment operator, ω is the photon energy, E is the energy of the initial hole i, $\mathrm{Im}\Sigma_i$ is the imaginary part of the self-energy of the initial hole i, ε is the energy of the primary photoelectron, g_{if} is the coupling strength for the electron-photon interaction which is given in the dipole approximation by

$$g_{if} = \langle i \,|\, r\cos\theta \,|\, f \rangle \, , \tag{2}$$

and $A_i(E)$ is the spectral function of the i hole which is given by

$$A_i(E) = \frac{1}{\pi} \mathrm{Im} G_i(E) \, . \tag{3}$$

The Green's function $G_i(E)$ of the i hole is given by

$$G_i(E) = [E - E_i^0 - \Sigma_i(E)]^{-1} \, . \tag{4}$$

The self-energy of the i hole $\Sigma_i(E)$ consists of the nonradiative part $\Sigma_i^{nx}(E)$ and the radiative part $\Sigma_i^{x}(E)$ which are to second order given by

$$\Sigma_i^{nx}(E) = \sum_{m,j,k} \frac{|\langle im \,|\, 1/r_{12} \,|\, jk \rangle|^2}{E_m^0 - E_j^0 - E_k^0 + E - i\delta} \, , \tag{5}$$

$$\Sigma_i^{x}(E) = \sum_{k} \frac{|g_{if}(\omega_k)|^2}{E + \omega_k - E_f^0 - i\delta} \, . \tag{6}$$

Here we consider only the renormalization of the nonradiative part of the self-energy by approximating the effective three-body [one-particle–two-holes, phh] interaction $I^{phh}(E)$ by the sum of the effective two-body interactions $I^{ph}(E)$ and $I^{hh}(E)$. The true three-body part $I^{phh}(E)$ only represents a small higher-order correction and may be neglected. The self-energy can be renormalized by introducing the effective hole-hole interaction $I^{hh}(E)$ to the intermediate holes j and k,

$$E_j^0 + E_k^0 \rightarrow E_{jk}(E) = E_j(E) + E_k(E) - I_{jk}^{hh}(E) \, . \tag{7}$$

The self-energy can be renormalized further by including the effective particle-hole interaction $I^{ph}(E)$. The self-energy is now obtained in the form

$$\Sigma_i(E) = \sum_{m,j,k} \frac{V_{jkim} \Gamma_{imjk}(E)}{E_m^0 - E_{jk}(E) + E - i\delta} \, , \tag{8}$$

with the effective interaction Γ_{imjk} given by a Bethe-Salpeter integral equation

$$\Gamma_{imjk}(E) = V_{imjk} + \sum_{m,j,k} \frac{[I_{jmjm'}^{ph}(E) + I_{kmkm'}^{ph}(E)] \Gamma_{im'jk}(E)}{E_m^0 - E_{jk}(E) + E - i\delta} \, . \tag{9}$$

The self-energy $\Sigma_i(E)$ can be divided into two parts corresponding to "static" relaxation and "dynamic" relaxation.[1] The static part is approximated by the monopole relaxation and since we are not going to consider any monopole shake-up or shake-off structure, we approximate it by the monopole relaxation energy shift.[1] The dynamic relaxation self-energy $\Sigma_i^{DR}(E)$ is evaluated using an extended version of the renormalized second-order expressions Eqs. (8) and (9) (Ref. 1),

$$\Sigma_i^{DR}(E) = \sum_{m,j,k} \frac{U_{jkim} \Gamma_{imjk}(E)}{E_m^0 - E_{jk}(E) + E - i\delta} \, , \tag{10}$$

$$\Gamma_{imjk}(E) = U_{imjk} + \sum_{m'} \frac{[I_{jmjm'}^{ph}(E) + I_{kmkm'}^{ph}(E)] \Gamma_{im'jk}(E)}{E_{m'}^0 - E_{jk}(E) + E - i\delta} \, , \tag{11}$$

where we note that U_{jkim} is defined to take into account important effects of time-reversed diagrams describing Fermi-sea correlation effects. We solve Eqs. (10) and (11) within the random-phase approximation with exchange (RPAE).[1] In this approximation the screening of the

electrostatic interaction between the particle and extra hole, and the relaxation of the excited electron, are neglected. This approximation becomes questionable when the variation of the continuum density is rapid and it breaks down for low-lying localized ionic excitations. The screening of the hole-hole repulsion $I^{hh}(E)$ is calculated in the static monopole approximation and the double-hole energy $E_{jk}(E)$ is obtained by the Dirac-Hartree-Fock ΔSCF method.

IV. NUMERICAL PROCEDURE

We discuss here briefly the numerical procedure used for the evaluation of the Green's function.

A. The final 4p-hole state

The dipolar fluctuation process involves correlation between angular distortions of atomic shells, where the $4p$ core hole and $4d$ charge densities correlate with each other by nonspherical dipolar distortions of the $4p$ and $4d$ charge densities. In the case of a $4p$ hole in the elements around Xe, this dipolar coupling is extremely strong.[1,5,6,8–10] In the present work we shall be particularly interested in the $4p^{-1}\leftrightarrow 4d^{-2}n(\varepsilon)f$ super-Coster-Kronig processes, $4p^{-1}\leftrightarrow 4d^{-1}5s^{-1}\varepsilon p$ and $4p^{-1}\leftrightarrow 4d^{-1}5p^{-1}\varepsilon d$ Coster-Kronig processes. In order to include contributions from the higher-order effects in Eq. (11), we calculate the wave functions for the excited electron m in a potential which directly includes a certain selection of the interaction matrix elements. The zeroth-order basis set will be chosen as follows.

(i) Occupied (hole) states: Free-neutral-atom Hartree-Fock (HF) ground-state orbitals.

(ii) Excited (particle) states: Two-core-hole (V^{N-2}) HF potential based on frozen ground-state orbitals.

The excited electron m is coupled to the core hole k to a ^1P total angular momentum state. The core hole j is a spectator, contributing only to the spherically symmetric Hartree

$$(j^{-1})_{\rm av}(k^{-1}m\ ^1P)\ \text{HF}\ V^{N-2}\ \text{potential}\ . \tag{12}$$

Using this basis is the same as working in the Tamm-Dancoff approximation with exchange (TDAE) for the $k^{-1}m$ dipole response and including the Hartree potential from the second hole j. The Fermi-sea correlation diagrams can now be expanded through the integral equation (11).

We also investigate another approximation as a zeroth-order orbital basis set for the $4p^{-1}\leftrightarrow 4d^{-2}n(\varepsilon)f$ super-Coster-Kronig (sCK) process.

(i) Occupied (hole) states: HF ground-state orbitals relaxed in the presence of one $4d$ or one $4p$ hole. We denote these orbitals by R_{4d} and R_{4p} in contrast to the frozen neutral-atom ground-state orbitals denoted by F.

(ii) Unoccupied (particle) states: Orbitals calculated in a HF V^{N-2} potential constructed using orbitals R_{4d} or R_{4p}, namely, the

$$(4d^{-1})_{\rm av}[4d^{-1}n(\varepsilon)f\ ^1P]\ \text{HF}\ V^{N-2}(R_{4d}\ \text{or}\ R_{4p})\ \text{potential}\ . \tag{13}$$

The RPAE approximation is used as in the frozen-core approximation. In Table I we summarize the combinations of basis sets used for the transition matrix elements.

Our motivation for using a relaxed-orbital approximation is as follows. For R_{4d}, the screening charge grows from zero to full strength while the Auger electron leaves the system; therefore the actual effect of relaxation on the potential corresponds to relaxation in the presence of half of a core hole, in addition to the core hole already present. In other words, using the completely relaxed final ionic state with two $4d$ holes will overestimate the influence of monopole-relaxation effects. From this viewpoint approximations 3 and 4 are used. In order to include the effect of the static monopole relaxation of the initial hole (a $4p$-hole state), approximations 2 and 5 are used. The effects of the monopole relaxation in the presence of one $4d$-hole state and those of one $4p$-hole state are almost the same. We found that the spectra calculated by approximations 2–5 are very similar.

B. The initial 2s-hole state

The dynamical (dipolar fluctuations) relaxation of the initial $2s$-hole level is also important. We consider the $2s^{-1}\leftrightarrow 2p^{-1}3d^{-1}(4d^{-1})\varepsilon f$ Coster-Kronig processes contribution in the same way as we considered the sCK processes for the final $4p$-hole state in calculating the $2s$-hole-state level.

In the present work the ground-state correlation energy shifts of the $4p$ and $4d$ levels are assumed to be a difference between the present Dirac-Hartree-Fock ΔSCF energy and the experimental hole energy[17] for the $4d$-hole level which is ≈ 1.0 eV. Also we neglected the radiative part of the self-energy, which is negligible for the present purpose.

V. RESULTS AND DISCUSSION

In Fig. 1 we show the present experimental and theoretical $L\gamma_{2,3}$ x-ray emission spectra of Xe. Note the following points.

(i) A good agreement between the calculated and experimental spectrum shows that the $L\gamma_{2,3}$ x-ray emission

TABLE I. The basis sets used in the calculations of the transition matrix elements.

Approximation	$4p$	$4d$	$4d$	$n(\varepsilon)f$
1	F	F	F	$V\ (F)$
2	F	F	F	$V\ (R_{4p})$
3	F	F	F	$V\ (R_{4d})$
4	R_{4p}	R_{4p}	R_{4p}	$V\ (R_{4p})$
5	R_{4d}	R_{4d}	R_{4d}	$V\ (R_{4d})$

spectrum of Xe can be interpreted essentially in terms of the corresponding $4p$-hole spectral function broadened by the spectral function of the initial $2s$ core hole which is assumed to be a Lorentzian profile. The effect of the initial $2s$-hole state on the final $4p$-hole state seems to be very small.

(ii) The energy position of the spectral peak (5306.7 eV), which was once assigned as the $4p_{3/2}^{-1}$ level, is well described by the present theory. The "$4p_{3/2}^{-1}$" XPS energy is 145.5 eV (Refs. 4 and 17) and the present theoretical XPS energy is 146.1 eV, in excellent agreement. The $2s$-hole energy determined by the present x-ray measurement is 5452.2 eV. Note that the $2s$-hole energy is shifted by 7.5 eV from the Dirac-Hartree-Fock [DHF ΔSCF energy (5459.7 eV)]. The initial $2s$-hole energy obtained by the present theory is 5452.8 eV, which is in excellent agreement with the present experimental $2s$-hole energy. For the present calculation we note that we used the experimental XPS $2s$-hole energy, which is 5453.2 eV.[18]

(iii) The prominent peak originates from mixing of a discrete $4p^{-1}$ level with a band of $4d^{-2}\varepsilon f$ excitations where f wave functions tend to localize resonantly in the region of the $4p$ and $4d$ orbitals, acquiring collapsed $4f$ character; therefore a substantial part (40%) of the $4p_{3/2}$ hole has gone into a kind of quasiparticle excitation in the form of a very compact mixture of $4p_{3/2}^{-1}$ and $4d^{-2}4f$ in Xe. The remaining part of the $4p_{3/2}$ core-hole strength and almost all of the $4p_{1/2}^{-1}$ core-level spectral strength have become spread over a large range of $4d^{-2}\varepsilon f$ continuum states. The quasiparticle picture of the final $4p$ core hole has now broken down completely and the final $4p$ core holes cease to exist as elementary excitations due to $4p^{-1}\leftrightarrow 4d^{-2}\varepsilon f$ super-Coster-Kronig process.

(iv) For the linewidth of the initial $2s$ hole we use the theoretical result by Chen *et al.*[19] who calculated the nonradiative lifetime by the relativistic Hartree-Fock-Slater basis set and the frozen-orbital approximation (different from the frozen-core approximation used here). The analysis of the width of the split-off level (the prominent peak) shows that the initial $2s$-hole linewidth is about 2.7 ± 0.4 eV (Ref. 20) which is smaller than the theoretical prediction (3.34 eV). The calculation by Chen *et al.*[19] tends to overestimate the width when the hole involves Coster-Kronig-type decay processes. This point was already pointed out by one of the authors and discussed in detail elsewhere.[21]

(v) In contrast to the frozen-core approximation (approximation 1), the relaxed-orbital approximations (approximations 2–5) give much better agreement with experiment above the $4d$ double-hole threshold.[22] This implies that the effect of the monopole relaxation of the surrounding charges on the Auger electron is substantial and not negligible. We have to note that the use of relaxed orbitals for the calculation of the transition matrix elements makes the approximation self-inconsistent from the viewpoint of perturbation theory as used in the present work.

VI. CONCLUDING REMARKS

The $L\gamma_{2,3}$ XES spectrum of Xe measured and calculated in the present work shows the breakdown of the quasiparticle picture of the $4p$ hole in Xe. The spectrum is essentially interpreted in terms of the spectral function of the final $4p$ hole. The effects of the initial $2s$-hole state on the final $4p$-hole state is small. In the present case the XES spectrum is well described in terms of the convolution of the spectral functions of the initial and final hole states. However, this can not be the case when a strongly interacting core hole like a $4p$ hole of Xe is involved as an initial hole in emission processes. The emission processes involving strongly interacting core holes are influenced by polarization of the charge density, which leads to screening of the emission matrix elements.[23] The direct x-ray fluorescence can be modulated by the "resonant" excitation and emission. This modulation leads to a pronounced interference effect between direct and induced emission. This strong interference effect in the electron-photon coupling strength (emission matrix element) lowers the decay rate of excited states.[23] As such an example the $4p$-$4d$ XES spectrum was studied theoretically by using the Green's-function method.[23] It was shown that inclusion of the screening of the emission vertex, i.e., screening of the electron-photon coupling in x-ray emission, will reduce the x-ray emission intensity in the initial ionic ground state and enhance the intensity in the initial ionic excited (satellite) states.[23]

ACKNOWLEDGMENTS

One of the authors (M.O.) is grateful to K. Ohno and S. J. Henke for help during the course of the present work. We would like to thank John W. Cooper for critical comments on the manuscript.

---

*Present address: Institut für Physikalische und Theoretische Chemie der Techischen Universität, Hans-Sommer-Strasse 10, Postfach 3329, D-3300 Braunschweig, West Germany.

[1]G. Wendin and M. Ohno, Phys. Scr. **14**, 148 (1976).

[2]G. Wendin, *Structure and Bonding* (Springer, Berlin, Heidelberg, New York, 1981), Vol. 45, p. 1; and references therein.

[3]L. S. Cederbaum, J. Schirmer, W. Domcke, and W. von Niessen, J. Phys. B. **10**, L549 (1977).

[4]U. Gelius, J. Electron Spectrosc. Relat. Phenom. **5**, 985 (1974).

[5]M. Ohno, Phys. Scr. **21**, 589 (1980).

[6]M. Ohno, J. Phys. C **13**, 447 (1980).

[7]R. E. LaVilla, Phys. Rev. A **17**, 1018 (1978).

[8]M. Ohno and G. Wendin, Solid State Commun. **39**, 875 (1981).

[9]M. Ohno and J-M Mariot, J. Phys. C **14**, L1133 (1981).

[10]M. Ohno (unpublished).

[11]R. D. Deslattes and B. Simson, Rev. Sci. Instrum. **37**, 753 (1966).

[12]R. D. Deslattes, E. G. Kessler, W. C. Sauder, and A. Henins,

Ann. Phys. (N.Y.) **129**, 378 (1980).
[13]R. D. Deslattes and R. E. LaVilla, Appl. Opt. **6**, 39 (1967).
[14]R. D. Deslattes, Rev. Sci. Instrum. **38**, 616 (1967).
[15]H. F. Beyer, R. D. Deslattes, F. Folkmann, and R. E. LaVilla, J. Phys. B **18**, 207 (1985).
[16]M. Ohno and G. Wendin, J. Phys. B **12**, 1305 (1979).
[17]S. Svensson, N. Mårtensson, E. Basilier, P. A. Malmquist, U. Gelius, and K. Siegbahn, Phys. Scr. **14**, 141 (1976).
[18]K. Siegbahn, C. Nordling, G. Johansson, J. Hedman, P. F. Heden, K. Hamrin, U. Gelius, T. Bergmark, L. O. Werme, R. Manne, and Y. Baer, *ESCA Applied to Free Molecules* (North-Holland, Amsterdam, 1969).
[19]M. H. Chen, B. Crasemann, and H. Marks, At. Data Nucl. Data Tables **24**, 13 (1979).
[20]The derived $2s$ hole linewidth was estimated by subtracting 1.05 eV the FWHM of the main line of the $4p$ XPS (Ref. 4) and 0.5 eV the FWHM of the crystal rocking curve from 4.2 ± 0.4 eV the FWHM of the peak in Fig. 1.
[21]M. Ohno and G. Wendin, Phys. Rev. A **31**, 2318 (1985).
[22]Calculated $4d$ double hole is 150.19 eV, corresponding to 5302.0 eV on Fig. 1.
[23]M. Ohno and G. Wendin, Z. Phys. D **5**, 233 (1987).